Effects of surface modification of noble-metal sensing electrodes with Au on the hydrogen-sensing properties of diode-type gas sensors employing an anodized titania film

Takeo Hyodo[*], Tomoki Yamashita, and Yasuhiro Shimizu

Graduate School of Engineering, Nagasaki University

1-14 Bunkyo-machi, Nagasaki 852-8521, Japan

*Corresponding author:

Takeo Hyodo, Dr.

Graduate School of Engineering, Nagasaki University

1-14 Bunkyo-machi, Nagasaki 852-8521, Japan

Tel: +81-95-819-2644

Fax: +81-95-819-2643

E-mail: hyodo@nagasaki-u.ac.jp

Abstract

Diode-type gas sensors employing an anodized TiO_2 film and noble-metal (Pt, Pd and Pd-Pt) sensing electrodes modified with and without a small amount of Au ($Au/M/TiO_2$ and M/TiO_2, respectively, M = Pt, Pd, Pd-Pt (Pd : Pt = 58 : 42 in weight)) have been fabricated, and the effects of surface modification of the electrodes with Au on their H_2-sensing properties have been investigated at 250°C in both air and N_2 under dry and wet atmospheres. H_2 response of all the M/TiO_2 sensors in N_2 was much larger than that in air under both dry and wet atmospheres. The Pt/TiO_2 sensor showed the smallest H_2 response in air among them, but the surface modification of the Pt electrode with Au was quite effective in enhancing the H_2 response of the Pt/TiO_2 sensor in air. Therefore, the response of the $Au/Pt/TiO_2$ sensor to 8000 ppm H_2 in air was comparable to that in N_2, especially under wet atmosphere, and thus the response of the $Au/Pt/TiO_2$ sensor to 8000 ppm H_2 was almost independent of oxygen concentration under wet atmosphere. In addition, the annealing of the sensor at 600°C did not affect the response of the $Au/Pt/TiO_2$ sensor to 8000 ppm H_2. The homogeneous mixing of Au into the Pt electrode also improved the H_2 response of the Pt/TiO_2 sensor, but the effectiveness was much lower than that of the surface modification of the Pt electrode with Au. On the other hand, the response of the as-fabricated $Au/Pd/TiO_2$ and $Au/Pd-Pt/TiO_2$ sensors to 8000 ppm H_2 in air were much larger than that of the $Au/Pd/TiO_2$ and $Au/Pd-Pt/TiO_2$ sensors annealed at 600°C, especially under wet atmosphere. The large H_2 response observed with the $Au/Pt/TiO_2$ sensor and the as-fabricated $Au/Pd/TiO_2$ and $Au/Pd-Pt/TiO_2$ sensors can be explained by large suppression of H_2 oxidation by Au components remained at the surface of their sensing electrodes and then increased amount of dissociatively-adsorbed hydrogen species at the sensing electrode surface.

1. Introduction

Numerous efforts have been directed to developing various kinds of highly sensitive and selective H_2 sensors [1-9], which were indispensable for operating next-generation power-supply systems utilizing H_2 as an energy source (e.g., fuel cells) as well as various industrial plants producing H_2 as a by-product (e.g., chlor-alkali electrolysis) safely and effectively. We have also demonstrated that sensing properties of various semiconductor-type H_2 sensors were improved by the strict control of mesopores and/or macropores of gas-sensing materials by utilizing self-assembly of surfactants in water [10-12] or polymer microspheres [13, 14] as a template as well as the control of sensor structure (especially, optimization of thickness and hetero-stacking of the sensing layer) by spin-coating [15-17], dipping [18] or slide-off transfer printing [19-21]. However, it is really difficult to operate the semiconductor-type H_2 sensors under O_2-free atmosphere, because the formation of negatively oxygen adsorbates on the oxide surface is essential for the reaction with the H_2 molecules. On the other hand, our interests have also been focused on the developing a diode-type H_2 sensor employing an anodized TiO_2 film and a sensing Pd electrode, because the sensor shows extremely large H_2 response even under O_2-free atmosphere as well as relatively excellent H_2 selectivity to other inflammable gases [22-25]. In addition, we have also reported that a diode-type H_2 sensor employing a Nb_2O_5 film fabricated by anodization of a Nb metal, in place of the anodized TiO_2 film, also showed the attractive H_2 response especially at low temperatures [26, 27], and the alloying of Pd with Pt was quite effective in improving the H_2 response and the long-term stability [28-30]. However, the H_2 response of the diode-type H_2 sensors was very sensitive to a change in oxygen concentration, and thus the magnitude of the H_2 response drastically increased with a decrease in the oxygen concentration. For example, we have reported that the H_2 response of these diode-type gas sensors in N_2 (i.e., ca. 0 vol% O_2) was about three orders of magnitude larger than that in air (i.e., 21 vol% O_2 in N_2) [24-26]. Therefore, we have attempted to decrease the large influence from O_2

concentration on the H_2 response by various techniques such as the alloying of Pd with Pt [28-30], the optimization of operating conditions (injection of moisture into the sample gas and drastic reduction in the applied forward bias [27-29]), and the coating of the surface of the noble-metal electrodes with various kinds of polymers [31-33]. However, these attempts had only limited effectiveness in reducing the influence from the O_2 concentration on the H_2 response. In this paper, therefore, the effects of surface modification of Pt, Pd and Pd-Pt electrodes with Au on the H_2 sensing properties of the diode-type gas sensors employing an anodized TiO_2 film have been investigated in both air and N_2 under dry and wet atmospheres. To confirm the role of Au, the effect the homogeneous mixing of Au into the Pt electrode on the H_2 sensing properties has also been tested.

2. Experimental

2.1 Fabrication of diode-type gas sensors

After a Ti plate ($5.0 \times 10.0 \times 0.5$ mm^3) was heat-treated at 600°C for 1 h in air, the half part of the Ti plate was anodized in 0.5 M H_2SO_4 aqueous solution at 20°C for 30 min at a current density of 50 mA cm^{-2}. A pair of noble-metal (Pt or Pd) electrodes was fabricated on the surface of both the TiO_2 thin film and the Ti plate by radio-frequency (rf) magnetron sputtering (Shimadzu, HSR-552S). The mixing of Pd or Au with Pt was also conducted by simultaneous deposition utilizing Pd and Pt targets or Pt and Au targets, which were denoted as Pd-Pt or Pt-nAu, n: the amount of Au (wt%), respectively. The composition of Pd-Pt and Pt-nAu was measured by electron dispersive X-ray spectroscopy (EDS, JEOL Ltd., JED-2300) equipped with scanning electron microscopy (SEM; JEOL Ltd., JSM-7500F). The ratio of Pd to Pt (Pd : Pt) of the Pd-Pt electrode was adjusted to 58 : 42 in weight, while the amount of Au (wt%) contained in the Pt electrode, n, of two kinds of Pt-nAu electrodes was *6* (Pt : Au = 94 : 6 in weight) or *16* (Pt : Au = 84 : 16 in weight).

In some cases, a small amount of Au was additionally deposited on the surface of the Pd, Pt, or Pd-Pt electrode by the rf magnetron sputtering. Each condition for the rf magnetron sputtering of noble metals is shown in Table 1, together with the thickness of the electrodes fabricated. Each electrode was connected with Au lead wire by using a Pt paste, and the electrical contact was ensured by firing at 600°C for 1 h in air. The obtained sensors with noble-metal electrodes modified with and without Au were denoted as $Au/M/TiO_2$ and M/TiO_2 (M: Pd, Pt, Pd-Pt, or Pt-nAu), respectively. The schematic drawing of the diode-type gas sensor obtained is shown in Fig. 1. The change in the chemical state of Au, Pd and Pt of the electrode surface was characterized by X-ray photoelectron spectroscopy using Al K_α radiation (XPS, Kratos, ACIS-TLATRA DLD), and the binding energy was calibrated using the C 1s level (284.5 eV) from usual contamination.

2.2 Measurements of H_2-sensing properties

A dc voltage of 100 mV was applied to the sensor under forward bias condition (M(+)-TiO_2-Ti(-)) and the sensing properties to 8000 ppm H_2 balanced with air or N_2 under dry or wet (absolute humidity (AH): 6.80, 9.40 or 12.8 g m^{-3}) atmospheres were measured at 250°C after annealing under the same gaseous condition at 600°C for 1 h. The magnitude of H_2 response was defined as "$I_g − I_b$", where I_g and I_b represented sensor-current values in 3~8000 ppm H_2 balanced with air or N_2 (at 10 min after the exposure to H_2) and in a base gas (air or N_2), respectively. 90% response time was defined as a period necessary to reach 90% sensor-current value of "$I_g − I_b$", while 90% recovery time was defined as that necessary to reach 90% sensor-current value of "$I_b − I_g$". Current (I)-voltage (V) characteristics of the sensors were also measured in an applied voltage range of -1.0 ~ +1.0 V in air or N_2 containing with and without 8000 ppm H_2 under dry or wet (AH: 6.80, 9.40 or 12.8 g m^{-3}) atmospheres at 250°C, after annealing under the same gaseous condition at 600°C for 1 h.

5

3. Results and Discussion

3.1 H$_2$-sensing properties of M/TiO$_2$ and Au/M/TiO$_2$ sensors (M: Pt, Pd and Pd-Pt) annealed at 600°C

Figure 2 shows *I-V* characteristics of annealed Pt/TiO$_2$ and Au/Pt/TiO$_2$ sensors in base gases (air and N$_2$) and in 8000 ppm H$_2$ balanced with the base gases under dry and the most humidified atmospheres (AR: 12.8 g m^{-3}) at 250°C. Both the sensors apparently showed nonlinear *I-V* characteristics under H$_2$-free and dry atmospheres, as shown in Fig. 2(a)(i). This behavior indicated that the Schottky barrier was formed at the interface between the electrode and the TiO$_2$ film. The forward current of both the sensors in dry air was extremely small even at a forward bias of +1.0 V (< 50 μA) due to the too high Schottky barrier, but an extreme reduction in oxygen concentration in the base gas (namely, dry N$_2$ atmosphere) drastically increased the forward current. The work function of Pt in dry N$_2$ is smaller than that in dry air, because the amount of O$_2$ molecules dissociated and then negatively adsorbed onto the Pt surface is small in comparison to those in dry air [34, 35]. Therefore, the height of the Schottky barrier at the electrode/TiO$_2$ interface in dry N$_2$ is smaller than that in dry air, and thus the amount of electrons transferred from TiO$_2$ to the electrode in dry N$_2$ are much larger than that in dry air under a forward bias. The surface modification of the Pt electrode with a small amount of Au slightly increased the forward current of the Pt/TiO$_2$ sensor in both dry air and N$_2$. This behavior shows that the surface modification with Au has little influence on the work function of Pt as well as the height of the Schottky barrier at the electrode/TiO$_2$ interface.

Variations in the *I-V* characteristics of the Pt/TiO$_2$ and Au/Pt/TiO$_2$ sensors induced by the addition of 8000 ppm H$_2$ into the dry atmospheres was largely affected by both the oxygen concentration in the sample gas and the surface modification with and without Au of the Pt electrode, as shown in Fig. 2(a)(ii). The addition of H$_2$ into dry air slightly increased the forward

current of the Pt/TiO$_2$ sensor, while that into dry N$_2$ drastically enhanced both the forward and reverse currents and the nonlinearity in the *I-V* curve almost collapsed, implying a large decrease in the height of the Schottky barrier at the electrode/TiO$_2$ interface. The increase in the sensor current induced by the H$_2$ addition into the dry atmosphere is due to dissociative adsorption of H$_2$ molecules on the Pt electrode, subsequent dissolution of the hydrogen species into the Pt electrode and in turn reduction of the Pt work function, leading to a decrease in the height of the Schottky barrier at the electrode/TiO$_2$ interface. Especially, the forward current of the Pt/TiO$_2$ sensor in dry N$_2$ containing 8000 ppm H$_2$ became larger than that in dry air containing 8000 ppm H$_2$ by three orders of magnitude. This indicates negligible consumption of H$_2$ at the Pt electrode in dry N$_2$, whereas a certain percentage of H$_2$ is likely consumed by the oxidation with oxygen adsorbates on the Pt surface in air. Thus the magnitude of the current of the Pt/TiO$_2$ sensor was quite sensitive to changes in the O$_2$ concentration under the atmosphere containing H$_2$. On the other hand, the surface modification of the Pt electrode with Au dramatically enhanced the forward current by ca. two orders of magnitude in dry air containing 8000 ppm H$_2$ with maintaining the nonlinear *I-V* characteristics. This indicated that the modified Au component largely inhibited the oxidation of H$_2$ molecules on the Pt surface and thus the amount of dissociatively-adsorbed hydrogen species drastically increased. The Schottky barrier at the electrode/TiO$_2$ interface perfectly disappeared in dry N$_2$ containing 8000 ppm H$_2$, and thus the Au/Pt/TiO$_2$ sensor showed linear *I-V* characteristics with the large current at low voltage (ca. +120 mA even at +300 mV). In addition, the effect of O$_2$ concentration on the magnitude of the forward current of the Au/Pt/TiO$_2$ sensor seems to be substantially smaller than that of the Pt/TiO$_2$ sensor, since the *I-V* characteristics of the Au/Pt/TiO$_2$ sensor in both dry air and N$_2$ containing 8000 ppm H$_2$ are in almost the same forward-current range.

The Pt/TiO$_2$ and Au/Pt/TiO$_2$ sensors showed nonlinear *I-V* characteristics also in most humidified air as well as N$_2$ (AH: 12.8 g m^{-3}) as shown in Fig. 2(b)(i). The forward current of

both the sensors in wet N_2 was much larger than that in wet air, as was observed with their *I-V* characteristics under dry H_2-free atmospheres. In addition, the surface modification of the Pt electrode with Au was relatively effective in increasing the forward current under wet H_2-free atmospheres in comparison with that under dry H_2-free atmosphere. Variations in the *I-V* characteristics of the Pt/TiO_2 and $Au/Pt/TiO_2$ sensors induced by the H_2 addition into wet air and N_2 (Fig. 2(b)(ii)) were roughly similar to those observed under dry air and N_2 atmospheres. Namely, 1) the forward current of all the sensors in both wet air and N_2 containing 8000 ppm H_2 was much larger than that in both wet H_2-free air and N_2, 2) the $Au/Pt/TiO_2$ sensor showed linear *I-V* characteristics in wet N_2 containing 8000 ppm H_2, and 3) the forward current of the $Au/Pt/TiO_2$ sensor was relatively larger than that of the Pt/TiO_2 sensor in both air and N_2 containing 8000 ppm H_2. However, the addition of H_2 into wet air drastically increased the reverse current of the $Au/Pt/TiO_2$ sensor and then the magnitude of the reverse current was saturated at around -0.03 A. In addition, the forward current of both the sensors in wet air containing 8000 ppm H_2 was larger than that in dry air containing 8000 ppm H_2, probably because water molecules inhibited the re-adsorption of O_2 molecules (i.e., the production of negatively-charged oxygen adsorbates) and thus the amount of dissociatively-adsorbed H_2 molecules relatively increased on the electrode surface. On the other hand, the addition of moisture into dry N_2 containing 8000 ppm H_2 reduced the forward current of both the sensors, probably because the adsorbed water molecules directly inhibited the dissociative adsorption of H_2 molecules. Therefore, the magnitude of the forward current of the $Au/Pt/TiO_2$ sensor in wet air containing 8000 ppm H_2 was comparable to that in wet N_2 containing 8000 ppm H_2. These results confirm that the $Au/Pt/TiO_2$ sensor shows the H_2 response less-dependent on oxygen concentration under wet atmosphere.

Figure 3 shows *I-V* characteristics of other annealed M/TiO_2 and $Au/M/TiO_2$ sensors (M: Pd and Pd-Pt) in air and N_2 containing 8000 ppm H_2 under dry and the most humidified

atmospheres (AH: 12.8 g m^{-3}) at 250°C. The *I-V* characteristics of these sensors under both dry and wet H$_2$-free atmospheres are not shown in this paper, but they were all nonlinear and the magnitude of the forward current of these sensors was almost comparable to that of the Pt/TiO$_2$ and Au/Pt/TiO$_2$ sensors under all gaseous atmospheres (see Fig. 2(a)(i) and Fig. 2(b)(i)). The forward current of the Pd/TiO$_2$ sensor was larger than that of the Pt/TiO$_2$ sensor under all H$_2$-containing atmospheres, because the amount of hydrogen solubility into Pd is generally much larger than that into Pt and thus the work function of Pd under the H$_2$-containing atmospheres is expected to be much smaller than that of Pt. The alloying of Pd with Pt (i.e., Pd-Pt) further enhanced the forward current of the Pd/TiO$_2$, especially in dry and wet air containing H$_2$, because the mixing of Pt into Pd reduced the coverage of oxygen adsorbates and/or the amount of PdO species on the electrode surface and thus promoted the dissociative adsorption of H$_2$ molecules and subsequent dissolution of the hydrogen species into the electrode, as reported in our previous study [30]. Both the Pd/TiO$_2$ and Pd-Pt/TiO$_2$ sensors showed entirely linear *I-V* characteristics and quite large forward current (several hundred mA at +1.0 V) in dry and wet N$_2$ containing H$_2$, and the alloying of Pd with Pt was hardly effective in enhancing the magnitude of current. The surface modification with Au enhanced the forward current of both the Pd/TiO$_2$ and Pd-Pt/TiO$_2$ sensors in dry and wet air containing 8000 ppm H$_2$, whereas the forward current of the Au/Pd/TiO$_2$ and Au/Pd-Pt/TiO$_2$ sensors in dry and wet N$_2$ containing 8000 ppm H$_2$ was almost comparable to that of the Pd/TiO$_2$ and Pd-Pt/TiO$_2$ sensors. These results show that the surface modification of the electrodes with Au was not effective enough in improving the oxygen dependence of the forward current of both the Pd/TiO$_2$ and Pd-Pt/TiO$_2$ sensors, in contrast to the case of the Pt/TiO$_2$ sensor.

Figure 4 shows response transients of the M/TiO$_2$ and Au/M/TiO$_2$ sensors (M: Pt, Pd and Pd-Pt, annealed at 600°C) to 8000 ppm H$_2$ in dry air and N$_2$ at 250°C at a forward bias of +100 mV. The Pt/TiO$_2$ sensor showed extremely low H$_2$ response (ca. 3.5 x 10^{-6} A) with overshooting

behavior and the H_2 response of the Pd/TiO$_2$ sensor (ca. 2.6 x 10^{-5} A) was slightly larger than that of the Pt/TiO$_2$ sensor in dry air. In addition, the alloying of Pd with Pt was effective in improving the H_2 response in dry air (ca. 1.8 x 10^{-4} A), and thus the Pd-Pt/TiO$_2$ sensor showed the largest H_2 response in dry air, among all the M/TiO$_2$ sensors, also as reported in our studies [28-33]. The H_2 response of these sensors in dry N_2 was extremely larger than that in dry air, as expected from their *I-V* characteristics (Figs. 2 and 3), and the ratio of the H_2 response in N_2 to that in air (Res_{N_2}/Res_{air}) under dry atmosphere was ca. 1.9 x 10^3, ca. 4.8 x 10^3 or ca. 3.1 x 10^2 for the Pt/TiO$_2$, Pd/TiO$_2$ or Pd-Pt/TiO$_2$ sensor, respectively. These results indicated that the H_2 response of all these sensors largely depended on oxygen concentration, but the alloying of Pd with Pt slightly decreased the influence of oxygen concentration on the H_2 response and the Res_{N_2}/Res_{air} of the Pd-Pt/TiO$_2$ sensor was the smallest among them. These effects of electrode components on the H_2 response were also well-coincident with those on the magnitude of forward current of their *I-V* characteristics (Figs. 2(a)(ii), 3(a)(i) and 3(b)(i)).

The surface modification of the M electrodes with Au drastically improved the H_2 response of some sensors, especially in dry air. Namely, the effects of the surface modification with Au enhanced were pronounced in the case of the pure Pt and Pt containing (i.e. Pd-Pt electrode) electrodes and then the magnitude of the H_2 response of the Au/Pt/TiO$_2$ sensor was three orders of magnitude larger than that of Pt/TiO$_2$ sensor in dry air. On the other hand, the surface modification of the M electrodes with Au was not sufficiently effective in improving the H_2 response of these sensors in dry N_2, in contrast to the case observed in dry air. The H_2 response of the Au/Pt/TiO$_2$ sensor was slightly larger than that of the Pt/TiO$_2$ sensor, while the H_2 response of the Au/Pd/TiO$_2$ and Au/Pd-Pt/TiO$_2$ sensors was slightly smaller than that of the Pd/TiO$_2$ and Pd-Pt/TiO$_2$ sensors, respectively, in dry N_2. Thus, it was confirmed that the surface modification with Au could enhance the H_2 response of Pt more effectively than that of Pd in dry air, and thus oxygen concentration dependence of the H_2 response could be reduced by the

surface modification with Au in the case of the pure Pt and Pt containing (i.e. Pd-Pt electrode) electrodes. Actually, the Res_{N_2}/Res_{air} of the Au/Pt/TiO$_2$ and Au/Pd-Pt/TiO$_2$ sensors (ca. 12 and ca. 15, respectively) was much smaller than that of the Au/Pd/TiO$_2$ sensor (2.6 x 10^2).

Response properties of the M/TiO$_2$ and Au/M/TiO$_2$ sensors (M: Pt, Pd and Pd-Pt, annealed at 600°C) to 8000 ppm H$_2$ in wet air and N$_2$ (AH: 6.8, 9.4 and 12.8 g m^{-3}) at 250°C were also measured at a forward bias of +100 mV, and the variations in the response of all the sensors to 8000 ppm H$_2$ with absolute humidity are summarized in Fig. 5, and the response transients of the M/TiO$_2$ and Au/M/TiO$_2$ sensors (M: Pt, Pd and Pd-Pt, annealed at 600°C) to 8000 ppm H$_2$ at a forward bias of +100 mV in representative wet air and N$_2$ (AH: 12.8 g m^{-3}) at 250°C are shown in Fig. 6. The H$_2$ response of these M/TiO$_2$ sensors in air gradually tended to increase with an increase in humidity, but the magnitude of H$_2$ response was extremely small even in the most humidified air, compared with that of these sensors in wet N$_2$. Among them, the Pt/TiO$_2$ sensor showed the smallest H$_2$ response under all wet air atmospheres. However, the surface modification of the Pt electrode with Au was quite effective in improving the H$_2$ response of the Pt/TiO$_2$ sensor in wet air as well as in dry air, and the H$_2$ response of the Au/Pt/TiO$_2$ sensor in air also gradually increased with an increase in humidity. The degree of the enhancement in the H$_2$ response of the Pt/TiO$_2$ sensor in N$_2$ induced by the surface modification with Au gradually decreased with an increase in humidity, and the H$_2$ response of the Au/Pt/TiO$_2$ sensor was comparable to that of the Pt/TiO$_2$ sensor in the most humidified N$_2$. Therefore, it was confirmed that the Au/Pt/TiO$_2$ sensor showed the excellent H$_2$ response which was scarcely dependent on oxygen concentration in wet N$_2$ (Res_{N_2}/Res_{air}: ca. 1.0 under the most humidified atmosphere) as shown in Figs. 5(a) and 6(a), as predicted also from their I-V characteristics (Fig. 2(b)(ii)). The oxygen concentration-independent H$_2$ response properties are considered to arise from the following reasons: 1) the Au component modified on the Pt electrode largely inhibited the oxidation of H$_2$ molecules on the sensing electrode and thus the amount of dissociatively-

adsorbed hydrogen species which dissolved into the electrode drastically increased in air, 2) the amount of the dissociatively-adsorbed hydrogen species on the sensing electrode decreased in wet N_2 by the adsorption of water molecules, and 3) the amount of oxygen adsorbates as well as the ratio of the amount of oxygen adsorbates to the amount of the dissociatively-adsorbed hydrogen species decreased with an increase in the humidity in air. On the other hand, the H_2 response of both the Pd/TiO$_2$ and Pd-Pt/TiO$_2$ sensors in wet air could not be enhanced effectively by the surface modification with Au. In addition, the H_2 response of both the Pd/TiO$_2$ and Pd-Pt/TiO$_2$ sensors slightly decreased by the surface modification with Au under all wet N_2 atmospheres. Therefore, the Res_{N_2}/Res_{air} of both the Au/Pd/TiO$_2$ and Au/Pd-Pt/TiO$_2$ sensors under wet atmospheres (ca. 290 and ca. 85 under the most humidified atmosphere, respectively) was much larger than that of the Au/Pt/TiO$_2$ sensor.

The surface modification of the Pt electrode with Au also affected the response and recovery behavior. Table 2 shows 90% response and recovery times of the Pt/TiO$_2$ and Au/Pt/TiO$_2$ sensors in air and N_2 under dry and the most humidified (AH: 12.8 g m^{-3}) atmospheres. The response and recovery speeds of the Pt/TiO$_2$ sensor in dry and wet air were relatively fast with the small H_2 response. In addition, the surface modification with Au reduced both the speeds with the large H_2 response, except for the recovery speed in dry air. The Au components on the Pt electrode surface may retard the rate of the reaction of H_2 molecules with oxygen adsorbates and/or the re-adsorption of O_2 molecules on the Pt electrode in air, leading to longer time to achieve steady-state conditions. The response and recovery speeds of the Pt/TiO$_2$ sensor in dry and wet N_2 were seriously slow, but the surface modification of the Pt electrode with Au drastically improved only the response speed of the Pt/TiO$_2$ sensor in dry and wet N_2. The fact may indicate that the surface modification with Au promotes the rate of the dissociative adsorption of H_2 molecules and/or the dissolution of hydrogen species into the Pt electrode. On the other hand, the response and recovery speeds of the Pd/TiO$_2$ and Pd/Pt/TiO$_2$ sensors

remained almost unchanged by the surface modification with Au.

3.2 Effects of the annealing conditions on H$_2$-sensing properties of Au/M/TiO$_2$ sensors (M: Pt, Pd and Pd-Pt)

Since the amount of Au modified on the M electrode was very low, the most Au atoms might migrate into the electrode, leading to alloying with Pd and Pt and then changing the composition and morphology of the electrode surface during the annealing process. Therefore, the H$_2$-sensing properties of the as-fabricated Au/M/TiO$_2$ sensors (M: Pt, Pd or Pd-Pt, only heat-treated at 250°C (operating temperature) for 1 h before the sensor measurement) were also measured at a forward bias of +100 mV in air and N$_2$ under dry and wet atmospheres at 250°C, and the variations in the response to 8000 ppm H$_2$ of the as-fabricated Au/M/TiO$_2$ sensors with absolute humidity are summarized in Fig. 7. For the comparative purpose, the data obtained with the annealed Au/M/TiO$_2$ sensors was plotted again in the same figure. The as-fabricated Au/Pt/TiO$_2$ sensor showed the H$_2$ response nearly identical to the annealed Au/Pt/TiO$_2$ sensor, but the H$_2$ response of the as-fabricated Au/Pt/TiO$_2$ sensor is slightly larger than that of the annealed Au/Pt/TiO$_2$ sensor in wet N$_2$ and thus the H$_2$ response of the as-fabricated Au/Pt/TiO$_2$ sensor was slightly dependent on oxygen concentration in wet N$_2$. Small differences in the composition and/or morphology of the surface of the Au/Pt electrodes between the as-fabricated and annealed Au/Pt/TiO$_2$ sensors may have a little influence on the adsorption state of hydrogen and/or oxygen adsorbates as well as water molecules in wet N$_2$. Surprisingly, the H$_2$ response of both the as-fabricated Au/Pd/TiO$_2$ and Au/Pd-Pt/TiO$_2$ sensors in air was much larger than that of the annealed Au/Pd/TiO$_2$ and Au/Pd-Pt/TiO$_2$ sensors in air, especially under wet atmosphere, and the magnitude of their H$_2$ response was quite comparable to that of the Au/Pt/TiO$_2$ sensor. Thus, the H$_2$ response of the as-fabricated Au/Pd/TiO$_2$ and Au/Pd-Pt/TiO$_2$ sensors was also nearly independent of oxygen concentration under wet atmosphere

(Res_{N_2}/Res_{air} of the as-fabricated Au/Pd/TiO$_2$ and Au/Pd-Pt/TiO$_2$ sensors under the most humidified atmosphere: ca. 3.8 and ca. 3.1, respectively)), as is the case with that of the Au/Pt/TiO$_2$ sensor. It is considered that the electrode surface of the as-fabricated Au/Pd/TiO$_2$ and Au/Pd-Pt/TiO$_2$ sensors was modified effectively with a small amount of Au, because they were not annealed at elevated temperatures. Therefore, the oxidation of H$_2$ with oxygen adsorbates largely limited on the Au-modified electrode surface and thus the amount of the dissociatively-adsorbed hydrogen species increased on the electrode surface, in comparison with Au-unmodified Pd and Pd-Pt electrodes. These are considered to be the possible reasons for large H$_2$ response in wet air observed for the as-fabricated Au/Pd/TiO$_2$ and Au/Pd-Pt/TiO$_2$ sensors.

3.3 Analysis of chemical states and depth profiles of Au/Pt and Au/Pd electrodes by XPS

All results obtained in sections 3.1 and 3.2 demonstrated that the effects of the surface modification of the electrodes with Au on the H$_2$-sensing properties are largely dependent on the difference of the main electrode composition (Pt or Pd). Therefore, the chemical states and depth profiles of the electrode materials (Au, Pt and Pd) of both Au/Pt/TiO$_2$ and Au/Pd/TiO$_2$ sensors as a representative were analyzed by XPS. Figures 8 and 9 show XPS spectra of Au and Pt, respectively, on the surface and in the bulk of the electrodes of the Au/Pt/TiO$_2$ sensors (i) as-fabricated, (ii) annealed at 600°C for 1 h in dry air and (iii) annealed at 600°C for 1 h in dry air, followed by at 600°C for 1 h in dry N$_2$. In addition, Fig. 10 shows XPS depth profiles of Au and Pt in the electrodes of these Au/Pt/TiO$_2$ sensors. Most of the Au and Pt on the surface of all the Au/Pt electrodes existed as a metal, irrespective of the different heat-treatment conditions, by referring to the binding energy reported in the literature [36]. However, the Au spectra on the electrode surface of the as-fabricated Au/Pt electrode shifted to lower binding energy (ca. 0.3 eV) and the intensity of the Au spectra largely reduced after annealing at 600°C. In addition,

the Au spectra of the as-fabricated Au/Pt electrode also shifted to lower binding energy with an increase in the etching depth, while that of other two Au/Pt electrodes annealed tended to slightly shift to higher binding energy with an increase in the etching depth. Bastl et al. reported that the XPS spectra of Au $4f_{7/2}$ of Au deposited on a Pt foil shifted to lower binding energy with a decrease in the Au coverage on the Pt surface (e.g., -0.78 eV for 0.01 monolayer-Au on Pt, -0.35 eV for 1 monolayer-Au on Pt) and more than 5 monolayer-stacking of Au atoms on the Pt surface was required to achieve the binding energy of Au bulk [37]. Berg et al. also demonstrated that the Au bulk showed the highest binding energy and isolated Au atoms showed a lower binding energy (ca. -0.3 eV for Au atoms deposited on Au surface (3 monolayer-stacked Au islands on Pt), -0.5 eV for Au atoms at the Au/Pt interface (1 monolayer-Au islands on Pt)) [38]. Considering the results of these previous studies, the XPS spectra of Au shown in Fig. 8 indicate that several ~ several tens of Au monolayers with bulk-like characteristics as a film or an island existed on the Pt surface and cluster-sized Au aggregates in the Pt bulk for the as-fabricated Au/Pt electrode. In addition, the size of Au aggregates is suggested to decrease with an increase in distance from the surface to the bulk. Both for the annealed two electrodes, however, highly-dispersed and/or 1~3 monolayer-stacked Au islands were suggested to exist even on the electrode surface. On the other hand, the Pt binding energy of the Au/Pt/TiO$_2$ electrode remained almost unchanged from the electrode surface to the balk, even after the annealing at elevated temperature. The asymmetric tail on the higher binding energy side of the Pt spectra of all the Au/Pt/TiO$_2$ electrodes is probably due to a shake-up effect, and the shape of all the asymmetric Pt spectra was independent of the annealing conditions as well as the depth from the surface of the electrode. Thus, no platinum oxide such as PtO was formed on the surface as well as bulk of the electrode. In addition, the ratio (R_{Au}) of Au to the total noble metals (Au+Pt) was ca. 30 at% even on the surface of the as-fabricated Au/Pt electrode, and it was smaller than the ratio (R_{Pt}) of Pt to the total noble metals on the

15

surface, ca. 70 at%. The R_{Au} drastically reduced within ca. 20 nm from the surface, and it mildly decreased with a further increase in the distance from the surface. The depth profile indicates that a small amount of Au apparently existed in the bulk of the electrode even though Au was merely sputtered on the surface of the Pt electrode. The reason for this result is not clear, but the Au sputtered on the Pt electrode, which was formed on the anodized TiO_2 film with quite large surface roughness [22-24, 28, 30] may migrate into the Pt electrode by heat of argon plasma in the rf magnetron sputtering. A similar tendency was confirmed also in the XPS depth profiles of the annealed Au/Pt electrodes, while the R_{Au} on the surface of both the Au/Pt electrodes annealed at 600°C was smaller than that of the as-fabricated Au/Pt electrode. It is considered that the small amount of Au components remained on the surface of the Au/Pt electrode even after the annealing at 600°C could play an important role in both limiting the oxidation of H_2 molecules on the electrode surface and increasing the dissociatively-adsorbed hydrogen species, and thus enhancing the H_2 response in air drastically, as discussed in sections 3.1 and 3.2.

On the other hand, the chemical states and depth profiles of Au and Pd of the Au/Pd electrode was largely different from those of the Au/Pt electrode after annealing at 600°C. Figures 11 and 12 show XPS spectra of Au and Pd, respectively, on the surface and in the bulk of the electrodes of the Au/Pd/TiO₂ sensors (i) as-fabricated, (ii) annealed at 250°C for 1 h in dry air, (iii) annealed at 600°C for 1 h in dry air and (iv) annealed at 600°C for 1 h in dry air, followed by at 600°C for 1 h in dry N_2. Figure 13 shows the XPS depth profiles of Au and Pt in the electrodes of these Au/Pd/TiO₂ sensors. Most of Au on the surface of all the Au/Pd electrodes was also metal. The binding energy of Au in the bulk of the as-fabricated electrode and the observable Au spectra on the surface as well as in the bulk of the annealed electrodes was also smaller than that on the surface of the as-fabricated electrode, as is the case with the Au/Pt electrodes. In addition, the XPS depth profiles of Au in the Au/Pd electrodes as-fabricated

16

and annealed at 250°C for 1 h in dry air were approximately similar to those in the Au/Pt electrodes as-fabricated and annealed at 600°C. Thus it was confirmed that a certain amount of Au remained on the surface of the Au/Pd electrode after annealing at 250°C. This may be a reason for the large H_2 response of the as-fabricated Au/Pd/TiO$_2$ sensor in air at 250°C, which was comparable to that of the Au/Pt/TiO$_2$ sensors as-fabricated and annealed at 600°C, as shown in Fig. 7. On the other hand, the Pd spectra of the Au/Pd electrodes as-fabricated and annealed at 250°C indicated that most of Pd in these Au/Pd electrodes existed as a metal but the a small amount of Pd on the surface and at the subsurface (etching depth: 3.2 nm) of the Au/Pd electrode might be oxidized to PdO because of slight increases in both the intensity of the asymmetric tail on the higher binding energy side and the half width of the Pd spectra. However, the annealing at 600°C in dry air perfectly oxidized the Pd to produce PdO on the electrode surface and the oxidation of Pd partly proceeded even in the bulk of the electrode, while Au on the electrode surface completely disappeared and the amount of Au slightly increased with an increase in the distance from the surface. In addition, the PdO was mostly reduced to Pd metal and a fraction of Au was observed on the surface as well as at every depth spot of the electrode, by the post annealing at 600°C in dry N_2 (Figs. 11(d) and 12(d)). Our previous study have demonstrated that submicron-sized Pd metal agglomerates were formed after annealing of a Pd film at 600°C in dry N_2 [28]. Therefore, the formation of large voids among such Pd metal agglomerates may enable us to obtain the XPS signal from Au in the electrode bulk without etching by Ar$^+$ sputtering. And therefore, this may the reason for the appearance of small and depth-independent Au spectra, as shown in Figs. 11(d) and 13(d). From these results, the considerably smaller H_2 response in air of the Au/Pd/TiO$_2$ sensor annealed at 600°C (see Figs. 4(b)(i), 5(b) and 6(b)(i)) than those of the as-fabricated Au/Pd/TiO$_2$ sensor as well as the as-fabricated and annealed Au/Pt/TiO$_2$ sensors can be explained by the following scenario: H_2 molecules are likely consumed at the outer surface of the Au/Pd electrode annealed at 600°C

by the reduction of PdO to Pd and then high catalytic activity of Pd itself due to disappearance of Au on the electrode surface and therefore the amount of dissolved hydrogen species into the electrode is expected to be reduced.

3.4 Effects of homogeneous mixing of Au into the Pt electrode on H_2-sensing properties of the Pt/TiO$_2$ sensor

Two kinds of Pt-nAu/TiO$_2$ sensors (n: *6* or *16*) were fabricated by utilizing simultaneous rf magnetron sputtering utilizing both Pt and Au targets, and their H_2-sensing properties after annealing at 600°C were measured at a forward bias of +100 mV in air and N_2 under dry and wet atmospheres at 250°C, to investigate the effects of Au addition into the bulk of the Pt electrode on the H_2-sensing properties. The variations in the response to 8000 ppm H_2 of the Pt-nAu/TiO$_2$ sensors (n: *6* or *16*) with absolute humidity are summarized in Fig. 14.   For comparative purpose, the data obtained with the Pt/TiO$_2$ sensor after annealing at 600°C is also plotted in the same figure. The addition of 6 wt% Au into the Pt electrode enhanced the H_2 response of the Pt/TiO$_2$ sensor under both air and N_2, but, the H_2 response of the Pt-6Au/TiO$_2$ sensor became lager than that of Pt/TiO$_2$ sensor, especially under air, and thus the Res_{N_2}/Res_{air} of the Pt-6Au/TiO$_2$ sensor became smaller than that of the Pt/TiO$_2$ sensor. In addition, the H_2 response of the Pt-6Au/TiO$_2$ sensor in N_2 was comparable to that of the Pt/Au/TiO$_2$ sensor (see Fig. 5(a)). However, the H_2 response of the Pt-6Au/TiO$_2$ sensor in air was smaller than that of the Au/Pt/TiO$_2$ sensor, indicating that the amount of Pt on the electrode surface of the Pt-6Au/TiO$_2$ sensor was larger than that on the electrode surface of the Au/Pt/TiO$_2$ sensor, due to the simultaneous deposition of both Au and Pt, and thus the oxidation of H_2 molecules easily proceeded on the Pt-6Au electrode in comparison with the Au/Pt electrode. Therefore, the effectiveness of the addition of Au to both the surface and bulk of the Pt electrode by the simultaneous sputtering was quite low in comparison with that of the surface modification of a

Pt electrode with a small amount of Au. The further increase in the amount of Au addition into the Pt electrode reduced the H_2 response of the Pt/TiO$_2$ sensor under all gaseous conditions in both air and N_2 under dry and wet atmospheres, and the Pt-*16*Au/TiO$_2$ sensor showed the large value of Res_{N_2}/Res_{air} (ca. 4.2 x 10^3 under the most humidified atmosphere), probably because the amount of both dissociative adsorption of H_2 molecules and dissolution of the hydrogen species into the electrode drastically reduced by too large amount of Au addition to the surface and the bulk of the Pt electrode. These results strongly supported that the surface modification of the Pt electrode with Au was quite effective in improving the H_2 response of the Pt/TiO$_2$ sensor, again.

3.5 Concentration dependence of H$_2$ response of the Au/Pt/TiO$_2$ sensor

Variations in H_2 response of the Au/Pt/TiO$_2$ sensor annealed at 600°C with H_2 concentration in air and N_2 under dry and wet (AH: 12.8 g m^{-3}) atmospheres and representative two response transients to H_2 are shown in Fig. 15. The magnitude of response to high-concentrated (8000 ppm) H_2 was less-dependent on the oxygen concentration, especially under wet atmosphere, also as shown in Figs. 4~6. This sensor showed extremely large H_2 response (over 10 mA, for more than 20 ppm H_2) in the all H_2 concentration range tested under both dry and wet N_2 atmospheres, and the addition of moisture decreased the H_2 response in the H_2 concentration range less than 10 ppm. However, the response value to 3 ppm H_2 in wet N_2 was relatively very large with maintaining the excellent signal to noise (S/N) ratio, as shown in Fig. 15(b). On the other hand, the H_2 response in dry air steeply decreased with a decrease in the H_2 concentration, while the H_2 response was improved in wet air, especially in the H_2 concentration range higher than 350 ppm. The lower limit for the H_2 detection under both dry and wet air atmospheres was ca. 20 ppm and it was much insensitive compared with that under both dry and wet N_2 atmospheres, and the S/N ratio of the response to low-concentrated H_2 was quite low, as shown

in Fig. 15(b). Therefore, oxygen concentration dependence of the H_2 response (i.e., Res_{N_2}/Res_{air})

increased with a decrease in the concentration of H_2 in a sample gas, because the ratio of the

amount of H_2 to be oxidized on the electrode to the initial concentration of H_2 in air increased

with a decrease in the initial concentration of H_2.

However, the effect of oxygen concentration on the H_2 response properties was tested only

at two points, i.e. 0% and 21% in volume, in the present study. Therefore, much more

investigations on both the H_2-sensing properties of the Au/Pt/TiO$_2$ sensor at various oxygen

concentrations between 0~21% in volume and the H_2-oxidation activity over the Au/Pt

electrode are presently required to understand the effects of the oxygen concentration on the

sensing mechanism accurately.

4. Conclusions

Effects of surface modification of noble-metal (M: Pt, Pd, or Pd-Pt) electrodes with Au on the

H_2-sensing properties of M/TiO$_2$ sensors mainly have been investigated at 250°C in air and N_2

under dry and wet atmospheres. H_2 response of all the M/TiO$_2$ sensors in N_2 was much larger

than that in air. The Pt/TiO$_2$ sensor showed the smallest H_2 response in air among all the M/TiO$_2$

sensors tested, but the surface modification of the sensing electrode with Au was quite effective

in enhancing the H_2 response of the Pt/TiO$_2$ sensor especially in wet air and then the Au/Pt/TiO$_2$

sensor showed the largest H_2 response among all the Au/M/TiO$_2$ sensors annealed at 600°C. Thus,

the H_2 response of the Au/Pt/TiO$_2$ sensor in wet air was comparable to that in wet N_2. In addition,

the similar effect of the surface modification with Au was confirmed also for H_2 response of all

the as-fabricated Au/M/TiO$_2$ sensors, but the homogeneous mixing of Au into the Pt electrode

was not effective in improving the H_2 response of the Pt/TiO$_2$ sensor, when it is compared with

case of the surface modification of the Pt electrode with Au. The XPS results indicated that a

certain amount of Au components remained on the electrode surface of the annealed Au/Pt/TiO$_2$

sensors and all the as-fabricated Au/M/TiO$_2$ sensors limited the oxidation of H$_2$ molecules and increased the dissociatively-adsorbed hydrogen species on the electrode surface, and thus enhanced the H$_2$ response in air drastically.

References

1. N. Yamazoe, New approaches for improving semiconductor gas sensors, Sens. Actuators B 5 (1991) 7-19.

2. J. Mizsei, How can sensitive and selective semiconductor gas sensors be made?, Sens. Actuators B 23 (1995) 173-176.

3. S. Zhuiykov, Hydrogen sensor based on a new type of proton conductive ceramic, Int. J. Hydrogen Energy 21 (1996) 149-759.

4. A. Katsuki and K. Fukui, H$_2$ selective gas sensor based on SnO$_2$, Sens. Actuators B 52 (1998) 30-37.

5. W. Shin, K. Tajima, Y. Choi, N. Izu, I. Matsubara, N. Murayama, Planar catalytic combustor film for thermoelectric hydrogen sensor, Sens. Actuators B 108 (2005) 455-460.

6. G. Korotcenkov, S. D. Han, J. R. Stetter, Review of electrochemical hydrogen sensors, Chem. Rev. 109 (2009) 1402-1433.

7. T. Watanabe, S. Okazaki, H. Nakagawa, K. Murata, K. Fukuda, A fiber-optic hydrogen gas sensor with low propagation loss, Sens. Actuators B 145 (2010) 781-787.

8. T. Hübert, L. Boon-Brett, G. Black, U. Banach, Hydrogen sensors – a review, Sens. Actuators B 157 (2011) 329-352.

9. S. A. Anggraini, M. Breedon, N. Miura, Zn-Ta-based oxide as a hydrogen sensitive electrode material for zirconia-based electrochemical gas sensors, Sens. Actuators B 187 (2013) 58-64.

10. T. Hyodo, N. Nishida, Y. Shimizu, M. Egashira, Preparation and gas-sensing properties of

thermally stable mesoporous SnO_2, Sens. Actuators B 83 (2002) 209-215.

11. G. S. Devi, T. Hyodo, Y. Shimizu, M. Egashira, Synthesis of mesoporous TiO_2-based powders and their gas-sensing properties, Sens. Actuators B 87 (2002) 122-129.

12. T. Hyodo, S. Abe, Y. Shimizu, M. Egashira, Gas sensing properties of ordered mesoporous SnO_2 and effects of coatings thereof, Sens. Actuators B 93 (2003) 590-600.

13. T. Hyodo, K. Sasahara, Y. Shimizu, M. Egashira, Preparation of macroporous SnO_2 films using PMMA microspheres and their sensing properties to NOx and H_2, Sens. Actuators B 106 (2005) 580-590.

14. K. Hieda, T. Hyodo, Y. Shimizu, M. Egashira, Preparation of porous tin dioxide powder by ultrasonic spray pyrolysis and their application to sensor materials, Sens. Actuators B 133 (2008) 144-150.

15. Y. Shimizu, Y. Nakamura, M. Egashira, Effects of diffusivity of hydrogen and oxygen through pores of thick film SnO_2-based sensors on their sensing properties, Sens. Actuators B 13-14 (1993) 128-131.

16. C.-D. Feng, Y. Shimizu, M. Egashira, Effect of microstructure of an SiO_2 thin film on the H2-sensing property of an SnO_2 sensor in an SiO_2/SnO_2 double-layered structure, Denki Kagaku (presently Electrochemistry) 61 (1993) 905‑906.

17. C.-D. Feng, Y. Shimizu, M. Egashira, Effect of gas diffusion process on sensing properties of SnO_2 thin film sensors in a SiO_2/SnO_2 layer-built structure fabricated by sol‑gel process, J. Electrochem. Soc. 141 (1994) 220‑225.

18. K. Wada, M. Egashira, Improvement of gas-sensing properties of a Pd/SnO_2 sensor by SiO_2 coating films formed by dipping method, J. Ceram. Soc. Jpn. 106 (1998) 84‑88.

19. A. Kawahara, H. Katsuki, M. Egashira, Fabrication of semiconductor oxide thick films by slide-off transfer printing and their NO2-sensing properties, Sens. Actuators B 49 (1998) 273‑278.

20. A. Kawahara, K. Yoshihara, H. Katsuki, Y. Shimizu, M. Egashira, Gas-sensing properties of semiconductor heterolayers fabricated by a slide-off printing method, Sens. Actuators B 65 (2000) 17‑22.

21. T. Hyodo, T. Mori, A. Kawahara, H. Katsuki, Y. Shimizu, M. Egashira, Gas-sensing properties of semiconductor heterolayer sensors fabricated by slide-off transfer printing, Sens. Actuators B 77 (2001) 41‑47.

22. Y. Shimizu, N. Kuwano, T. Hyodo, M. Egashira, High H_2 sensing performance of anodically oxidized TiO_2 Film contacted with Pd, Sens. Actuators B 83 (2002) 195-201.

23. T. Iwanaga, T. Hyodo, Y. Shimizu, M. Egashira, H_2 sensing properties and mechanism of anodically oxidized TiO_2 film contacted with Pd Electrode, Sens. Actuators B 93 (2003) 519-525.

24. T. Hyodo, T. Iwanaga, Y. Shimizu, M. Egashira, Effects of electrode materials and oxygen partial pressure on the hydrogen sensing properties of anodically oxidized titanium dioxide films, ITE Letters, 4 (2003) 594-597.

25. H. Miyazaki, T. Hyodo, Y. Shimizu, M. Egashira, Hydrogen-sensing properties of anodically oxidized TiO_2 film sensors: effects of preparation and pretreatment conditions, Sens. Actuators B 108 (2005) 467-472.

26. T. Hyodo, J. Ohoka, Y. Shimizu, M. Egashira, Design of anodically oxidized Nb_2O_5 films as a diode-type H_2 sensing material, Sens. Actuators B 117 (2006) 359-366.

27. T. Hyodo, H. Shibata, Y. Shimizu, M. Egashira, H_2 sensing properties of diode-type gas sensors fabricated with Ti- and/or Nb-based materials, Sens. Actuators B 142 (2009) 92-104.

28. Y. Shimizu, K. Sakamoto, M. Nakaoka, T. Hyodo, M. Egashira, H_2 sensing performance of TiO_2-based diode-type sensors, Adv. Mater. Res. 47-50 (2008) 1510-1513.

29. M. Nakaoka, T. Hyodo, Y. Shimizu, M. Egashira, Hydrogen sensing properties of an

anodized TiO$_2$ film equipped with a Pd-Pt electrode, ECS Trans. 16(11) (2008) 317-323.

30. T. Hyodo, M. Nakaoka, Y. Shimizu, and M. Egashira, Diode-type H$_2$ sensors using anodized TiO$_2$ films -structural and compositional controls of noble metal sensing electrodes, Sensor Letters 9 (2011) 641-645.

31. T. Hyodo, M. Nakaoka, Y. Shimizu, M. Egashira, Diode-type gas sensors fabricated with a titania film on a Ti plate and Pd-Pt electrodes -effects of polymer coating on the hydrogen-sensing properties-, IOP Conference Series: Materials Science and Engineering 18 (2011) 212006.

32. G. Yamamoto, T. Yamashita, K. Matsuo, T. Hyodo, Y. Shimizu, Diode-type sensors fabricated with anodized TiO$_2$ films equipped with Pd-Pt electrodes: effects of polytetrafluoroethylene or polyimide coating on their H$_2$ sensing properties, Sens. Actuators B 183 (2013) 253-264.

33. T. Hyodo, G. Yamamoto, K. Kamada, Y. Shimizu, Improvements in H$_2$-sensing properties of diode-type gas sensors using anodized TiO$_2$ films and Pd-Pt electrodes –polymer coating on the electrodes II–, Chemical Sensors, in press.

34. C. S. Shern, Changes in work function of hydrogen and oxygen adsorption on Pt(110) surface measured by mirror electron microscope-LEED, Chinese Journal of Physics, 30(6), pp. 841-850 (1992).

35. N. Guillet, A. Rives, R. Lalauze, C. Pijolat, Study of adsorption of oxygen on β-Al$_2$O$_3$ + Au and β-Al$_2$O$_3$ + Pt work function measurements – proposition of a model, Appl. Surf. Sci. 210 (2003) 286-292.

36. C. D. Wagner, W. M. Riggs, L. E. Davis, J. F. Moulder, G. E. Muilenberg, Handbook of X-ray Photoelectron Spectroscopy, Perkin-Elmer Corp., Minnesota (1978).

37. Z. Bastl, Š Pick, Angle resolved X-ray photoelectron spectroscopy study of Au deposited on Pt and Re surface, Surf. Sci. 566-568 (2004) 832-836.

38. C. Berg, H. J. Venvik, F. Strisland, A. Borg, Nucleation and growth of Au overlayers on Pt(100)-hex-R0.7° studied by STM and photoelectron spectroscopy, Surf. Sci. 409 (1998) 1-15.

Figure Captions

Fig. 1.　(a) Top and (b) cross-sectional schematic drawings of a diode-type gas sensor.

Fig. 2.　*I-V* characteristics of annealed Pt/TiO_2 and $Au/Pt/TiO_2$ sensors in base gases (air and N_2) and in 8000 ppm H_2 balanced with the base gases under dry and the most humidified atmospheres (AR: 12.8 g m^{-3}) at 250°C.

Fig. 3.　*I-V* characteristics of M/TiO_2 and $Au/M/TiO_2$ sensors (M: Pt, Pd and Pd-Pt, annealed at 600°C) in air and N_2 containing 8000 ppm H_2 under dry and the most humidified atmospheres (AR: 12.8 g m^{-3}) at 250°C.

Fig. 4.　Response transients of M/TiO_2 and $Au/M/TiO_2$ sensors (M: Pt, Pd and Pd-Pt, annealed at 600°C) to 8000 ppm H_2 at a forward bias of +100 mV in dry air and N_2 at 250°C.

Fig. 5.　Variations in the response to 8000 ppm H_2 of M/TiO_2 and $Au/M/TiO_2$ sensors (M: Pt, Pd and Pd-Pt, annealed at 600°C) with absolute humidity at 250°C.

Fig. 6.　Response transients of the M/TiO_2 and $Au/M/TiO_2$ sensors (M: Pt, Pd and Pd-Pt, annealed at 600°C) to 8000 ppm H_2 at a forward bias of +100 mV in wet air and N_2 (AH: 12.8 g m^{-3}) at 250°C.

Fig. 7.　Variations in the response to 8000 ppm H_2 of as-fabricated $Au/M/TiO_2$ sensors (M: Pt, Pd and Pd-Pt, just heat-treated at 250°C (operating temperature) for 1 h before the sensor measurement) with absolute humidity at 250°C, together with those of the $Au/M/TiO_2$ sensors annealed at 600°C.

Fig. 8.　XPS spectra of Au on the surface and in the bulk of the electrodes of the $Au/Pt/TiO_2$ sensors (i) as-fabricated, (ii) annealed at 600°C for 1 h in dry air and (iii) annealed at 600°C for 1 h in dry air, followed by at 600°C for 1 h in dry N_2.

Fig. 9.　XPS spectra of Pt on the surface and in the bulk of the electrodes of the $Au/Pt/TiO_2$ sensors (i) as-fabricated, (ii) annealed at 600°C for 1 h in dry air and (iii) annealed at 600°C for 1 h in dry air, followed by at 600°C for 1 h in dry N_2.

Fig. 10. XPS depth profiles of Au and Pt in the electrodes of the Au/Pt/TiO$_2$ sensors (i) as-fabricated, (ii) annealed at 600°C for 1 h in dry air and (iii) annealed at 600°C for 1 h in dry air, followed by at 600°C for 1 h in dry N$_2$.

Fig. 11. XPS spectra of Au on the surface and in the bulk of the electrodes of Au/Pd/TiO$_2$ sensors (i) as-fabricated, (ii) annealed at 250°C for 1 h in dry air, (iii) annealed at 600°C for 1 h in dry air and (iv) annealed at 600°C for 1 h in dry air, followed by at 600°C for 1 h in dry N$_2$.

Fig. 12. XPS spectra of Pd on the surface and in the bulk of the electrodes of Au/Pd/TiO$_2$ sensors (i) as-fabricated, (ii) annealed at 250°C for 1 h in dry air, (iii) annealed at 600°C for 1 h in dry air and (iv) annealed at 600°C for 1 h in dry air, followed by at 600°C for 1 h in dry N$_2$.

Fig. 13. XPS depth profiles of Au and Pd in the electrodes of Au/Pt/TiO$_2$ sensors (i) as-fabricated, (ii) annealed at 250°C for 1 h in dry air, (iii) annealed at 600°C for 1 h in dry air and (iv) annealed at 600°C for 1 h in dry air, followed by at 600°C for 1 h in dry N$_2$.

Fig. 14. Variations in the response to 8000 ppm H$_2$ of the Pt-nAu/TiO$_2$ sensors (n: *6* or *16*) with absolute humidity, together with that of the Pt/TiO$_2$ sensor annealed at 600°C.

Fig. 15. (a) Variations in H$_2$ response of the Au/Pt/TiO$_2$ sensor annealed at 600°C with H$_2$ concentration in air and N$_2$ under dry and wet (AH: 12.8 g m^{-3}) atmospheres and (b) representative two response transients to H$_2$.

Table 1.   Sputtering conditions and thickness of electrodes of all sensors.

Sensor	Power to target / W (Time / s)			Thickness of electrode / nm
	Pd	Pt	Au	
Pd/TiO$_2$	300 (1080)		-	287
Pt/TiO$_2$	-	300 (480)	-	78
Pd-Pt/TiO$_2$	300 (180)	200 (180)	-	177
Au/Pd/TiO$_2$	300 (300)	-	40 (10)	111
Au/Pt/TiO$_2$	-	300 (360)	40 (10)	84
Au/Pd-Pt/TiO$_2$	300 (180)	200 (180)	40 (10)	79
Pt-6Au/TiO$_2$	250 (300)	-	40 (300)	138
Pt-16Au/TiO$_2$	200 (600)	-	80 (300)	310

Table 2.   90% response and recovery times of Pt/TiO$_2$ and Au/Pt/TiO$_2$ sensors in air and N$_2$ under dry and the most humidified (AH: 12.8 g m^{-3}) atmospheres.

Sensor	90% response time / min				90% recovery time / min			
	Dry		Wet		Dry		Wet	
	Air	N$_2$	Air	N$_2$	Air	N$_2$	Air	N$_2$
Pt/TiO$_2$	0.42	5.58	0.68	7.19	1.29	2.28	1.03	2.12
Au/Pt/TiO$_2$	1.42	0.46	1.58	1.05	0.68	2.92	2.22	3.97
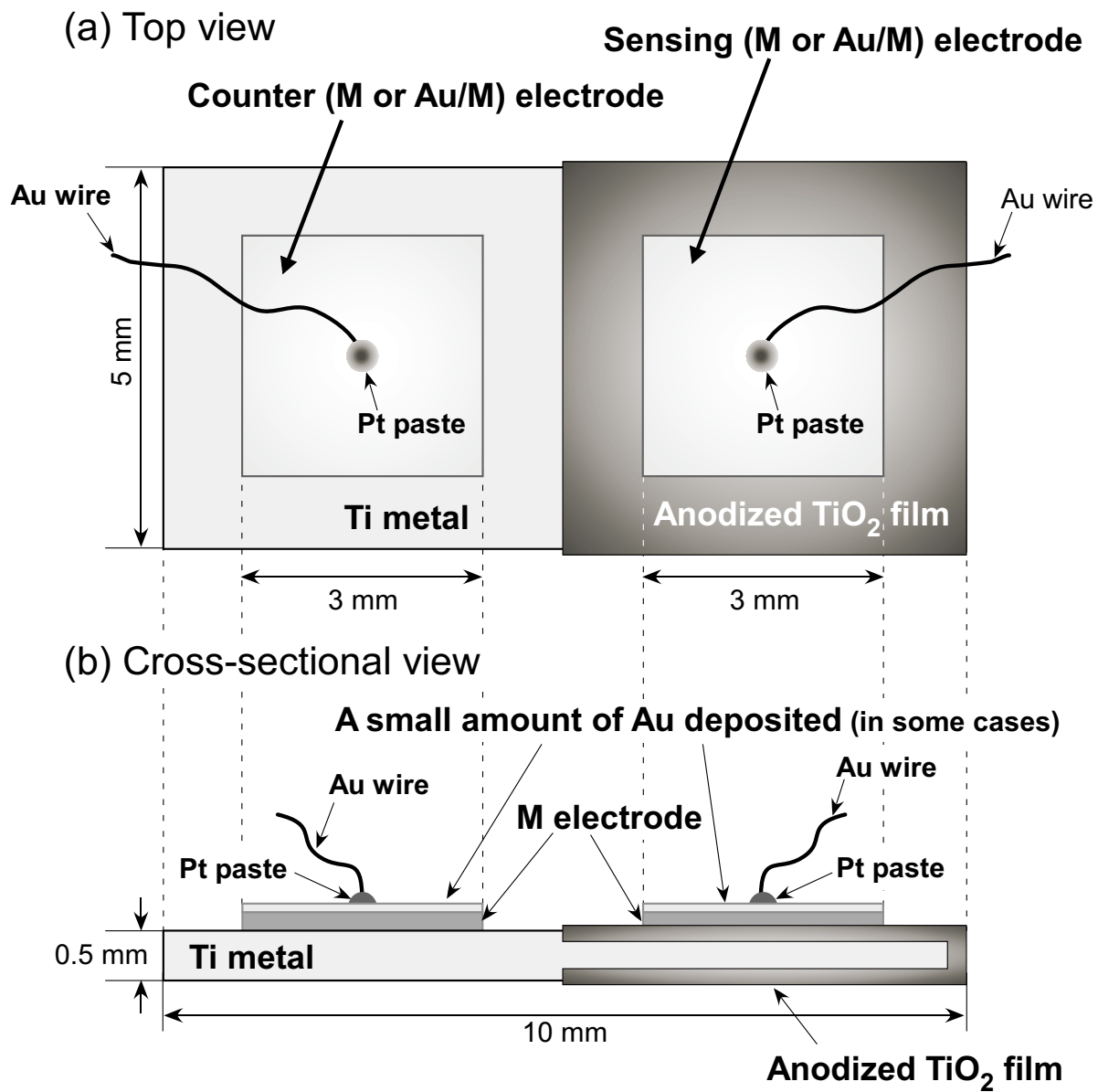
(a) Top view

Counter (M or Au/M) electrode

Sensing (M or Au/M) electrode

Au wire

Au wire

5 mm

Pt paste

Pt paste

Ti metal

Anodized TiO$_2$ film

3 mm

3 mm

(b) Cross-sectional view

A small amount of Au deposited (in some cases)

Au wire

Au wire

M electrode

Pt paste

Pt paste

0.5 mm

Ti metal

10 mm

Anodized TiO$_2$ film

Fig. 1. Hyodo et al.

Fig. 2. Hyodo et al.

(a) M = Pd

(i) Dry H₂

(ii) Wet H₂

(b) M = Pd-Pt

(i) Dry H₂

(ii) Wet H₂
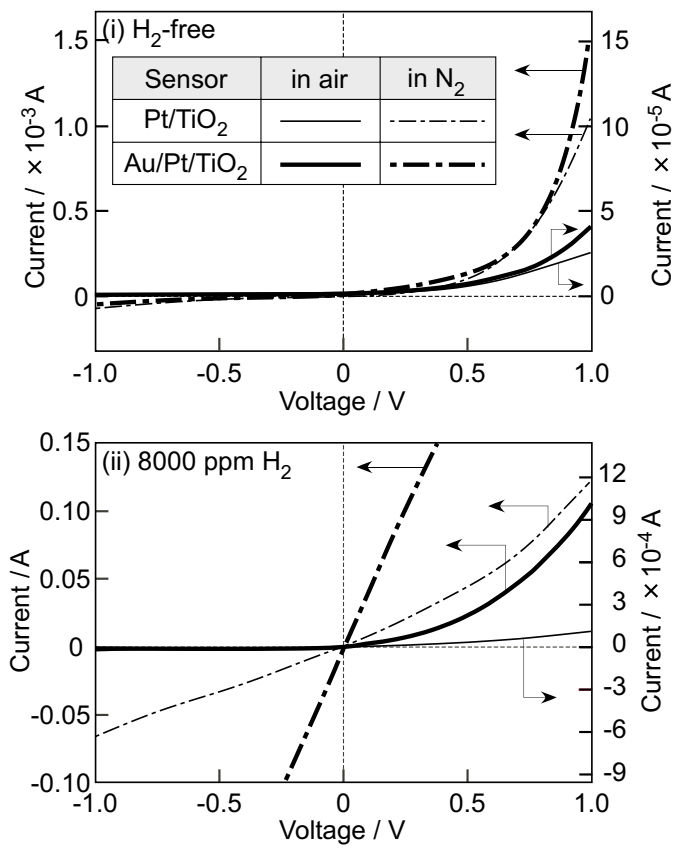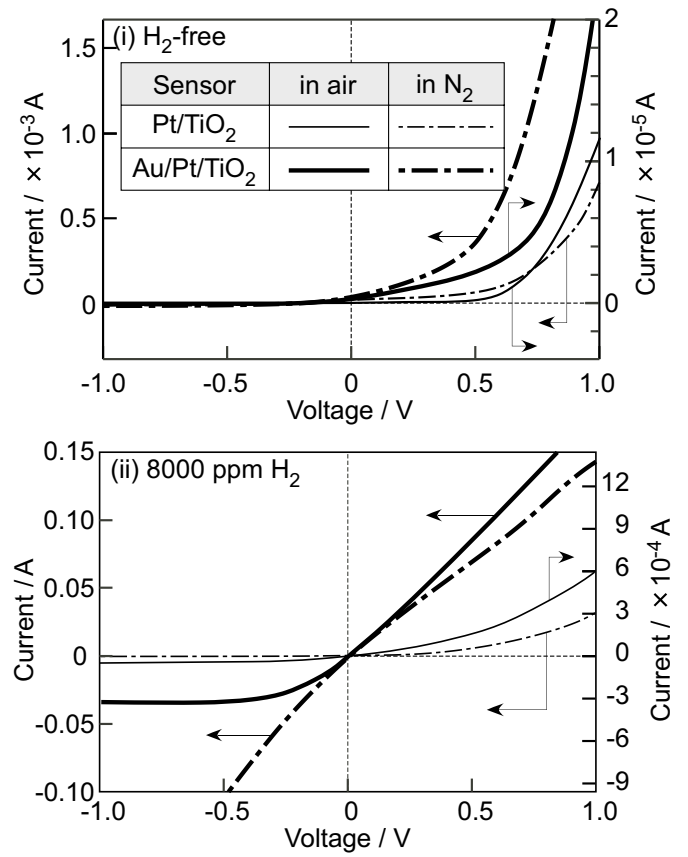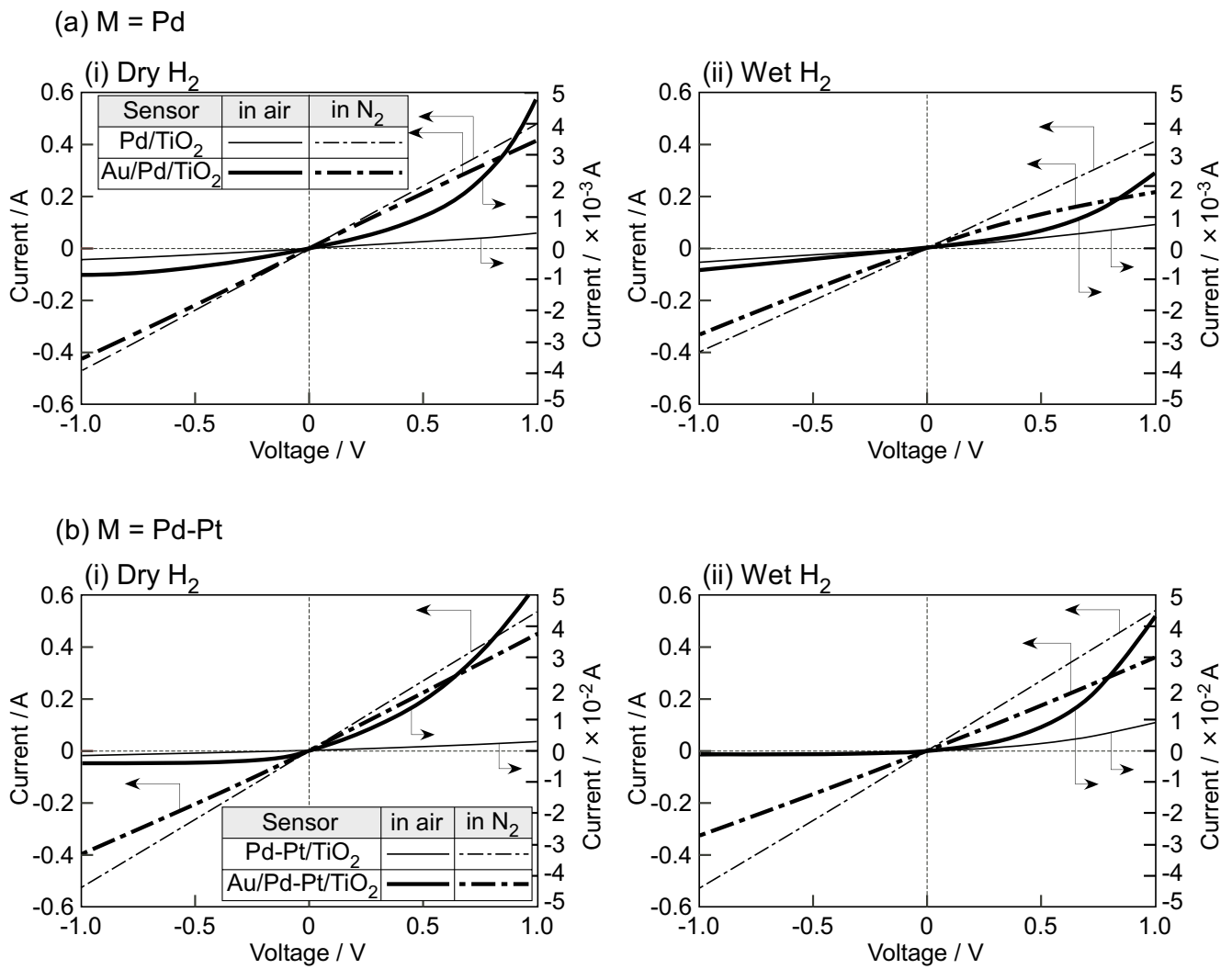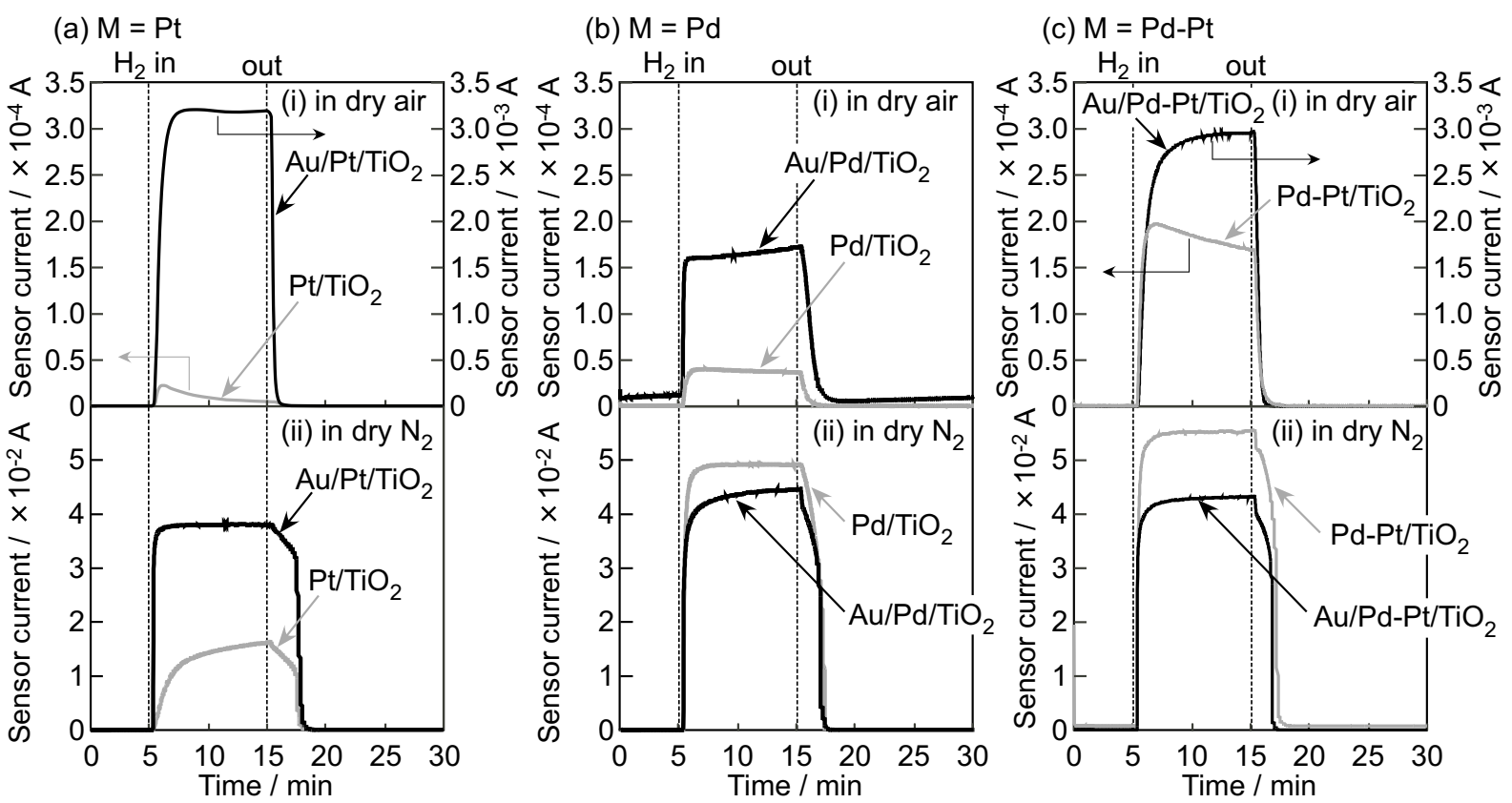
Fig. 3. Hyodo et al.

Fig. 4. Hyodo et al.
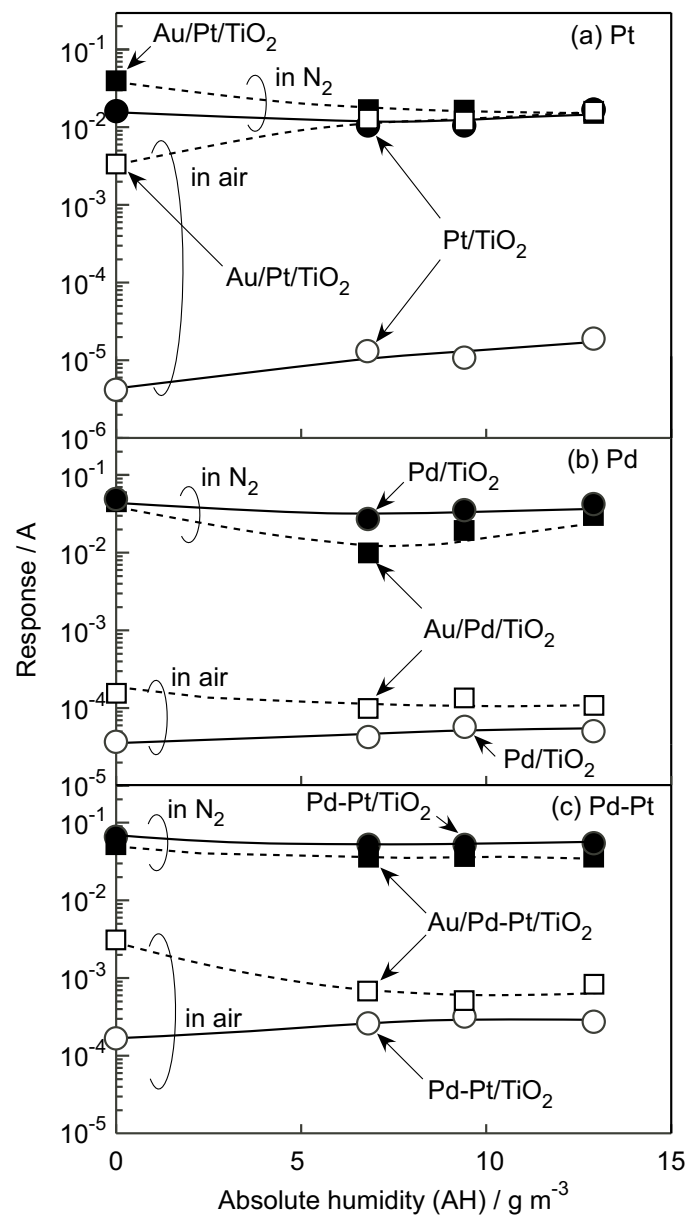
Fig. 5. Hyodo et al.
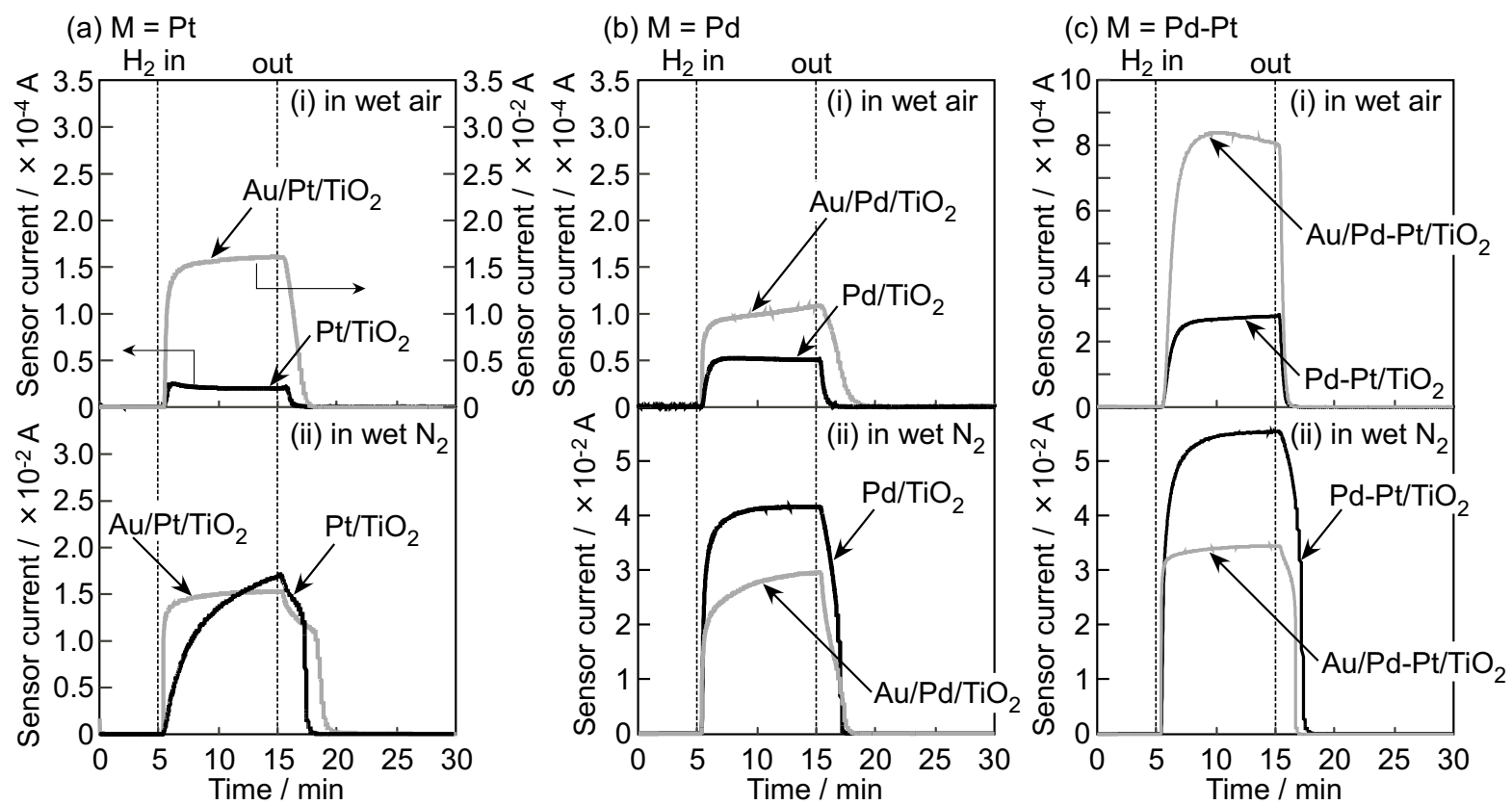
Fig. 6. Hyodo et al.
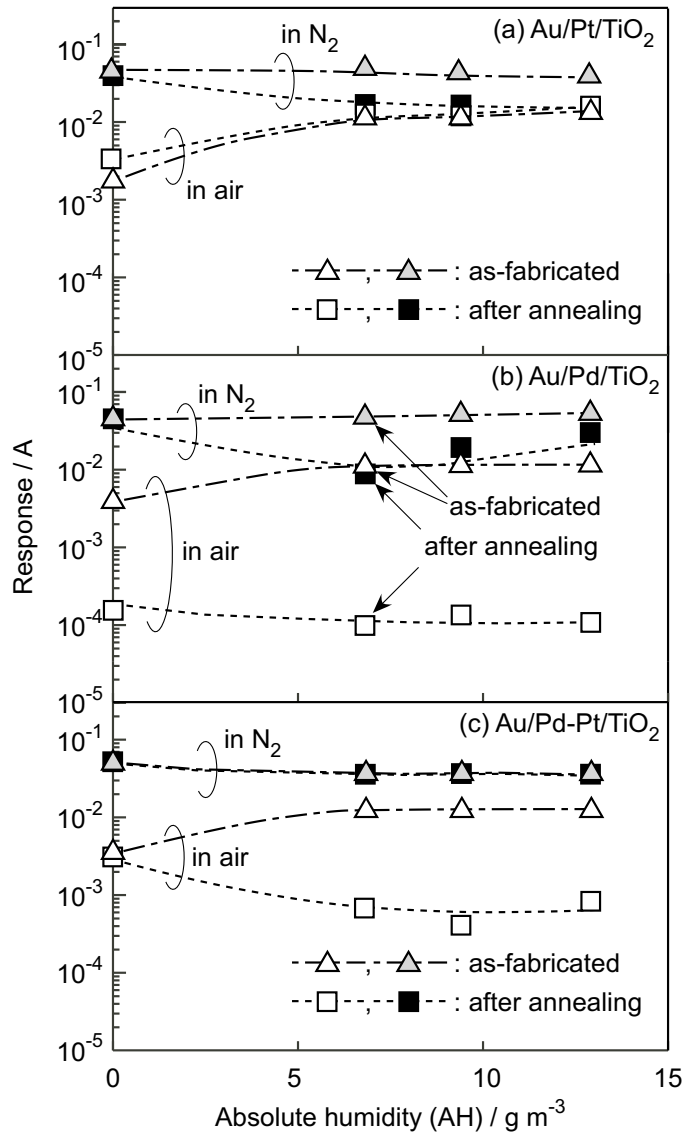
Fig. 7. Hyodo et al.
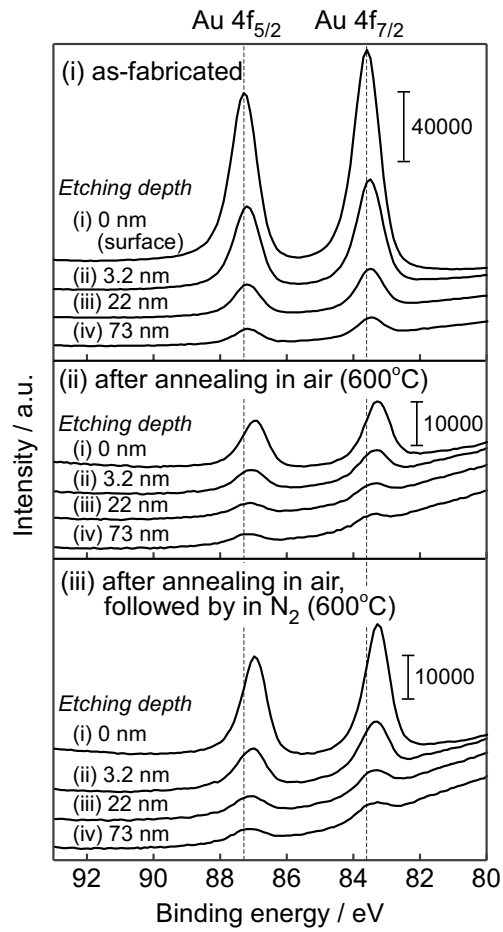
Fig. 8. Hyodo et al.
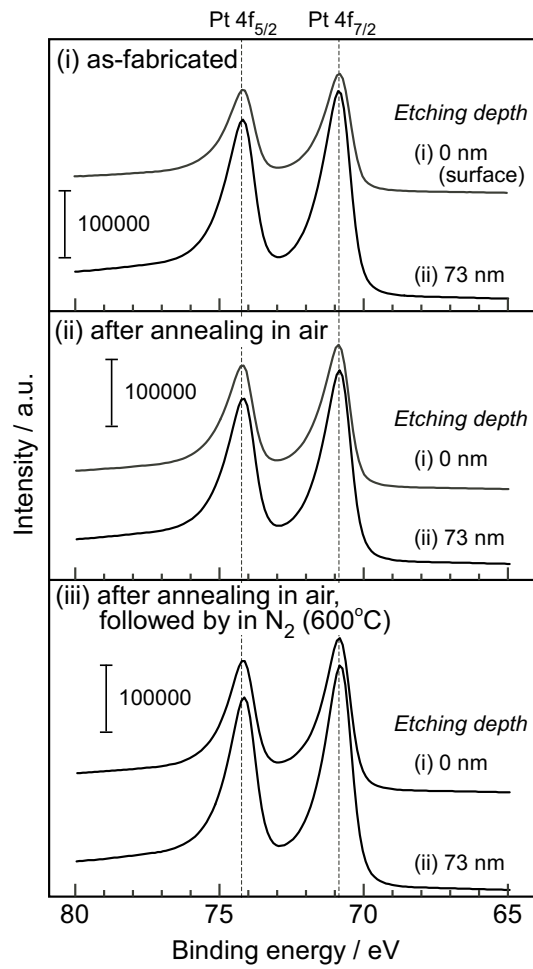
Fig. 9. Hyodo et al.
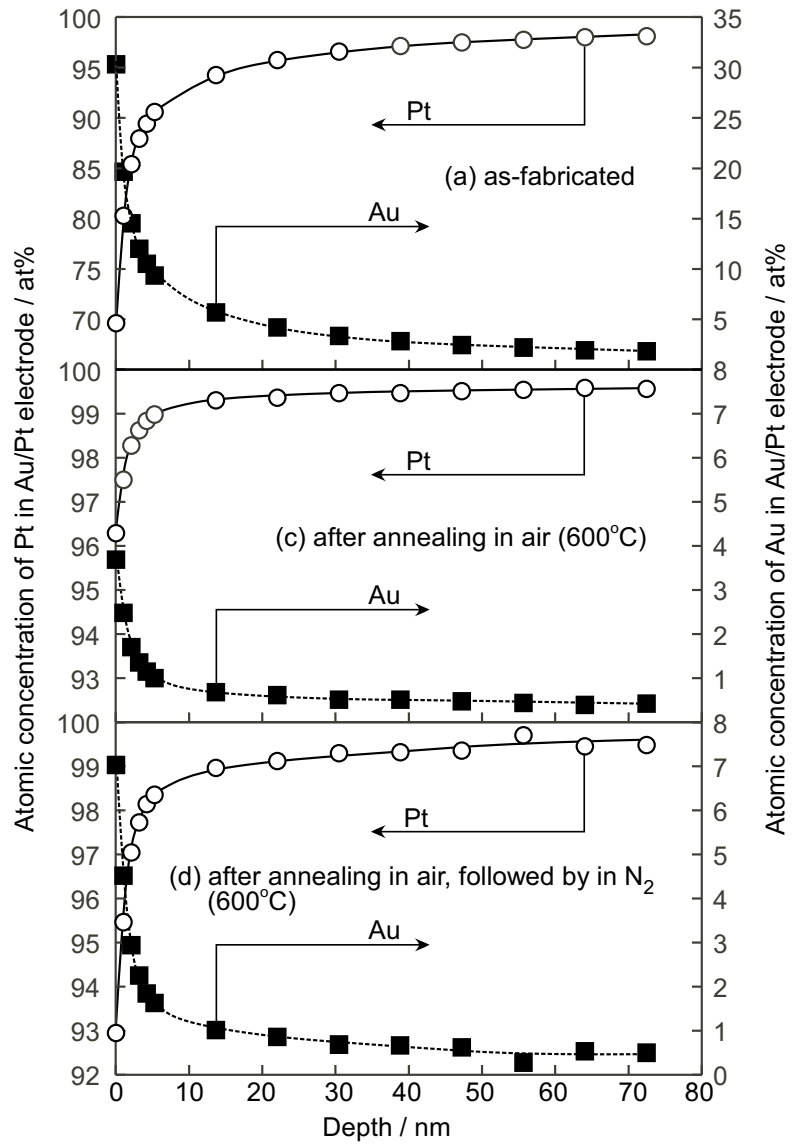
Fig. 10. Hyodo et al.
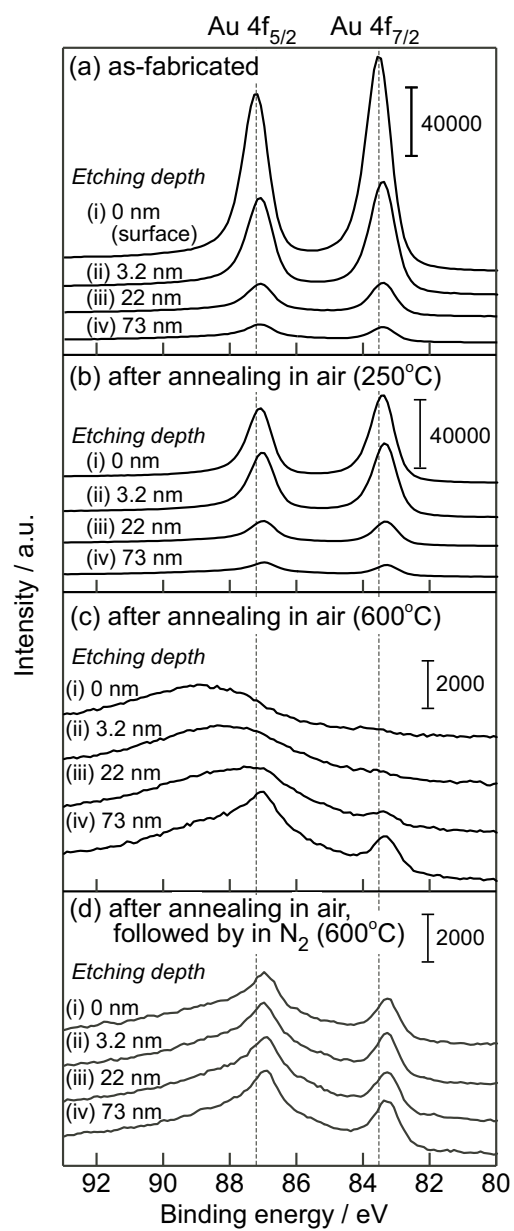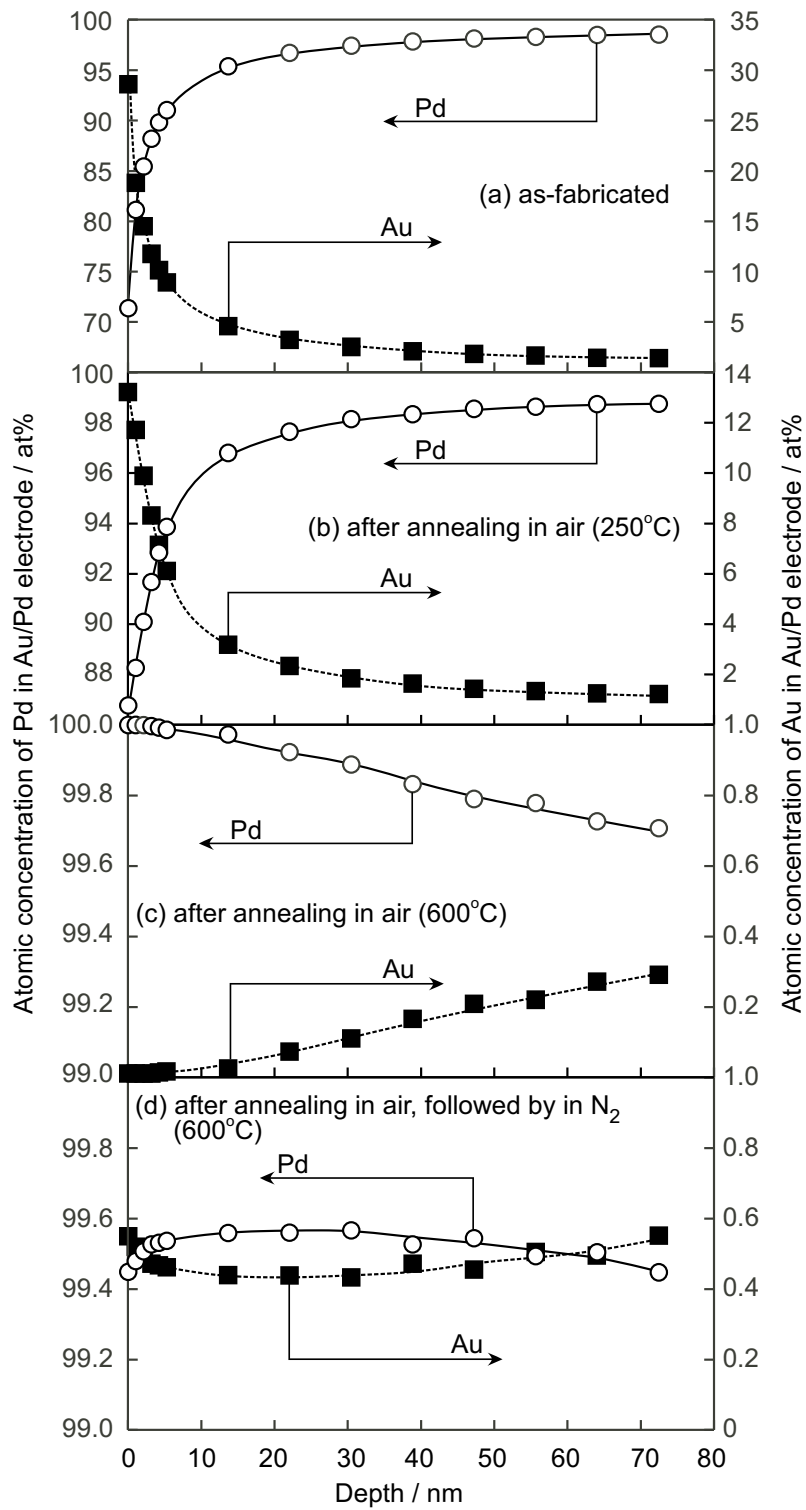
Fig. 11. Hyodo et al.
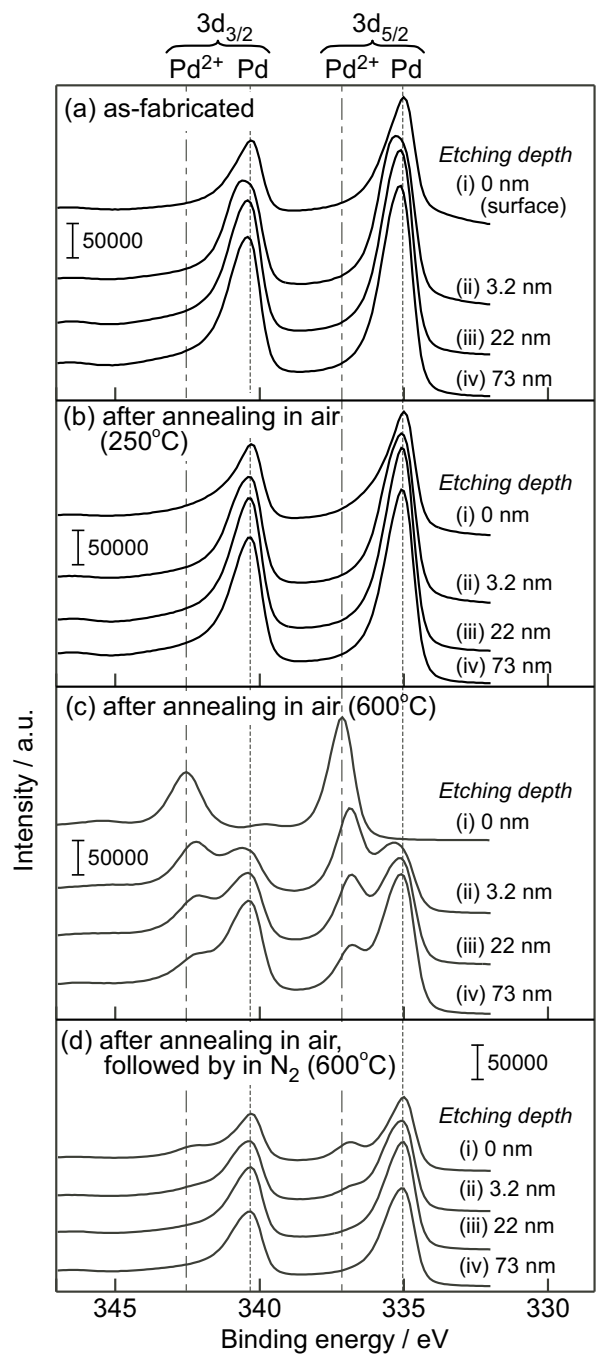
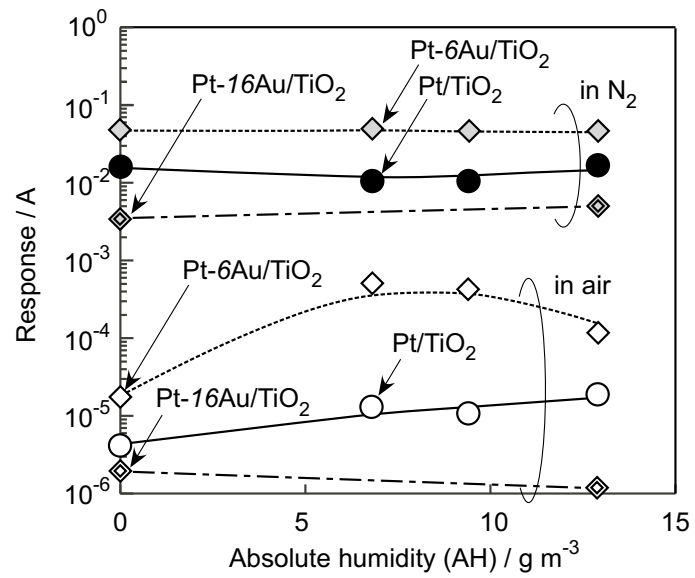Fig. 12. Hyodo et al.

Fig. 13. Hyodo et al.
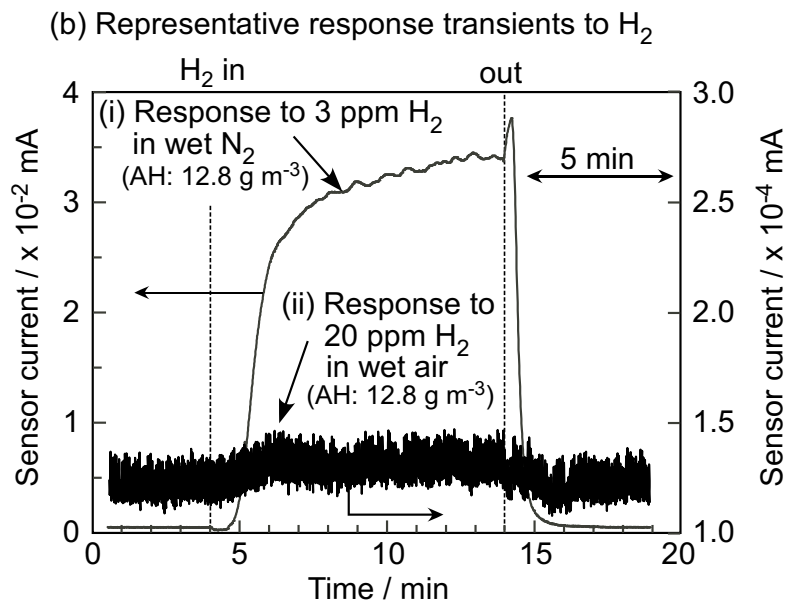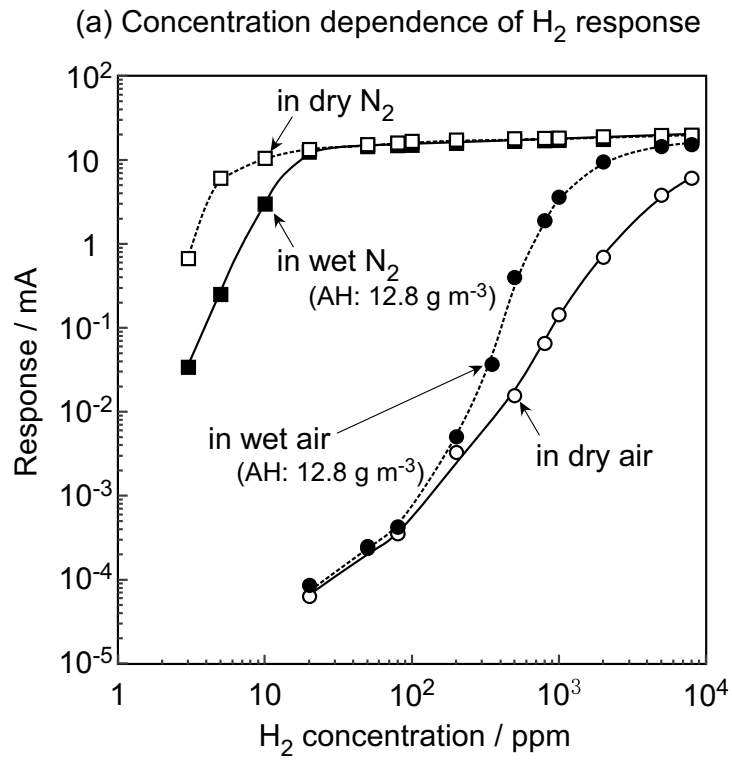
Fig. 14. Hyodo et al.

(a) Concentration dependence of H$_2$ response

(b) Representative response transients to H$_2$

Fig. 15. Hyodo et al.